physical sciences forum

MDPI

Proceeding Paper

The Morphology of the Active Galactic Nucleus and its Impact on Accretion Flows and Relativistic Jets †

Mohammed B. Al-Fadhli

College of Science, University of Lincoln, Lincoln LN6 7TS, UK; malfadhli@lincoln.ac.uk or mo.fadhli7@gmail.com

† Presented at the 2nd Electronic Conference on Universe, 16 February–2 March 2023; Available online: https://ecu2023.sciforum.net/.

Abstract: The G2 gas cloud motion data and the scarcity of observations on the event horizon-scale distances have challenged the comprehensiveness of the central supermassive black hole model. In addition, the recent Planck Legacy 2018 release has confirmed the existence of an enhanced lensing amplitude in the cosmic microwave background power spectra, which prefers a positively curved early Universe with a confidence level higher than 99%. This study investigates the impact of the background curvature and its evolution over conformal time on the formation and morphological evolution of central compact objects and the consequent effect on their host galaxies. The formation of a galaxy from the collapse of a supermassive gas cloud in the early Universe is modelled based on interaction field equations as a 4D relativistic cloud-world that flows and spins through a 4D conformal bulk of a primordial positive curvature considering the preference of the Planck release. Owing to the curved background, the derived model reveal that the galaxy and its core are formed at the same process by undergoing a forced vortex formation with a central event horizon leading to opposite vortices (traversable wormholes) that spatially shrink while evolving in the conformal time. The model shows that the accretion flow into the supermassive compact objects only occurs at the central event horizon of the two opposite vortices while their other ends eject relativistic jets. The simulation of the early bulk curvature evolution into the present spatial flatness demonstrated the fast orbital speed of outer stars owing to external fields exerted on galaxies. Furthermore, the gravitational potential of the early curved bulk contributes to galaxy formation while the present spatial flatness deprives the bulk potential which can contribute to galaxy quenching. Accordingly, the model can explain the relativistic jet generation and the G2 gas cloud motion if its orbit is around one of the vortices but at a distance from the central event horizon. Finally, the formation of a galaxy and its core simultaneously could elucidate the growth of the supermassive compact galaxy cores to a mass of ~10^9 $M_\odot$ at $\leq$ 6% of the current Universe age.

Keywords: galaxy formation; conformal spacetime; brane-world modified gravity

Citation: Al-Fadhli, M.B. The Morphology of the Active Galactic Nucleus and its Impact on Accretion Flows and Relativistic Jets. *Phys. Sci. Forum* **2023**, *7*, 52. https://doi.org/10.3390/ECU2023-14026

Academic Editor: Mauro D'Onofrio

Published: 15 February 2023

1. Introduction

Relativistic jets are extended beams of ionized matter that are emitted in opposite directions along the axis of rotation of active galaxies, quasars, stellar black holes, neutron stars and pulsars at speeds that approach the speed of light. Their radiative signatures and kinetic luminosity can be immensely powerful and such jets can exceed thousandths to millions of parsecs in length. The precise mechanisms by which the relativistic jets are produced are under ongoing debate in the scientific community [1–3].

The Planck Legacy 2018 (PL18) release has confirmed the presence of an enhanced lensing amplitude in the CMB power spectra, which prefers a positively curved early Universe with a confidence level higher than 99% [4,5]. Besides, efforts to reconcile this lensing amplitude with spatial flatness by using baryon acoustic oscillation data were challenged due to a tension of 2.5 to 3σ in the curvature parameter between these data [6].

In contrast, the positively curved early Universe naturally explains the anomalous lensing amplitude, aid a large-scale cut-off in primaeval density fluctuations [4] and agrees with the low CMB anisotropy observations [7,8].

This study presents a new galaxy formation concept by utilizing interaction field equations in which celestial objects are deemed as 4D relativistic cloud-worlds that flow and spin through a 4D conformal bulk of a primordial positive curvature considering the preference of PL18 release. The derived model reveals a new mechanism of relativistic jet generation.

2. Interaction Field Equations

The PL18 release has preferred a positively curved early Universe, that is, is a sign of a primordial background curvature or a curved bulk. To incorporate the bulk curvature and its evolution over the conformal time, a modulus of spacetime deformation, E_D in terms of energy density, is utilized [9]. The modulus can be expressed in terms of the field strength of the bulk by using the Lagrangian formulation of the energy density existing in the bulk as a manifestation of the vacuum energy density as follows:

$$E_D = \frac{T_{\mu\nu} - T g_{\mu\nu}/2}{R_{\mu\nu}/\mathscr{R}} = \frac{-\mathscr{F}_{\lambda\rho}\mathscr{F}^{\lambda\rho}}{4\mu_0} \tag{1}$$

where $\mathscr{F}_{\lambda\rho}$ is the field strength tensor of the bulk and μ_0 is the vacuum permeability. By incorporating the bulk influence, the Einstein–Hilbert action can be extended to:

$$S = E_D \int_C \left[\frac{R}{\mathscr{R}} + \frac{L}{\mathscr{L}}\right] \sqrt{-g}\, d^4\rho \tag{2}$$

where R is the Ricci scalar curvature representing a localized curvature induced in the bulk by a celestial object that is regarded as a 4D relativistic cloud-world of metric g_{uv} and Lagrangian density L respectively. $\mathscr{R}$ is the scalar curvature of the 4D conformal bulk of metric $\widetilde{g}_{\mu\nu}$ whereas $\mathscr{L}$ is the bulk's Lagrangian density. By considering the expansion of the bulk, a dual-action concerning the conservation of energy on global (bulk) and local (cloud-world) scales can be introduced as:

$$S = \int_B \left[\frac{-\mathscr{F}_{\lambda\rho}\widetilde{g}^{\lambda\gamma}\mathscr{F}_{\gamma\alpha}\widetilde{g}^{\rho\alpha}}{4\mu_0}\right] \sqrt{-\widetilde{g}} \int_C \left[\frac{R_{\mu\nu}g^{\mu\nu}}{\mathscr{R}_{\mu\nu}\widetilde{g}^{\mu\nu}} + \frac{L_{\mu\nu}g^{\mu\nu}}{\mathscr{L}_{\mu\nu}\widetilde{g}^{\mu\nu}}\right] \sqrt{-g}\, d^4\rho\, d^4\sigma \tag{3}$$

Applying the principle of stationary action in Ref. [10] yields:

$$\frac{R_{\mu\nu}}{\mathscr{R}} - \frac{1}{2}\frac{R}{\mathscr{R}}g_{\mu\nu} - \frac{R\mathscr{R}_{\mu\nu}}{\mathscr{R}^2} + \frac{R\left(\mathscr{K}_{\mu\nu} - \frac{1}{2}K\hat{p}_{\mu\nu}\right) - \mathscr{R}\left(K_{\mu\nu} - \frac{1}{2}K\hat{q}_{\mu\nu}\right)}{\mathscr{R}^2} = \frac{\hat{T}_{\mu\nu}}{\mathscr{T}_{\mu\nu}} \tag{4}$$

These interaction field equations can be interpreted as indicating that the cloud-world's induced curvature over the bulk (background) curvature equals the ratio of the cloud-world's imposed energy density and its flux to the bulk's vacuum energy density and its flux in the expanding/contracting Universe. By comparing Equation (1) with Einstein field equations and then transforming intrinsic, $\mathscr{R}_{\mu\nu}$, and extrinsic, $\mathscr{K}_{\mu\nu}$, curvatures of the bulk in Ref. [10], the equations can be simplified to:

$$R_{\mu\nu} - \frac{1}{2}R\hat{g}_{\mu\nu} - \left(K_{\mu\nu} - \frac{1}{2}K\hat{q}_{\mu\nu}\right) = \frac{8\pi G_{\mathscr{R}}}{c^4}\hat{T}_{\mu\nu} \tag{5}$$

where $\hat{g}_{\mu\nu} = g_{\mu\nu} + 2\mathscr{R}_{\mu\nu}/\mathscr{R} - 2\overline{\overline{g}}_{\mu\nu}$ or can be expressed as $\hat{g}_{\mu\nu} = g_{\mu\nu} + 2\widetilde{g}_{\mu\nu} - 2\overline{\overline{g}}_{\mu\nu}$ because $\mathscr{R}_{\mu\nu}/\mathscr{R} = \mathscr{R}_{\mu\nu}/\mathscr{R}_{\mu\nu}\widetilde{g}^{\mu\nu} = \widetilde{g}_{\mu\nu}$, is the conformally transformed metric counting for the contribution of the cloud-world metric, $g_{\mu\nu}$, in addition to the contributions from the intrinsic and extrinsic curvatures of the bulk, whereas Einstein spaces are a subclass of

conformal spaces [11]. The evolution in the effective $G_{\mathscr{R}}$ reflects the field strength of the bulk and depends on its curvature.

3. Galaxy Formation and Relativistic Jet Generation

The entire contribution comes from the boundary term when calculating the black hole entropy using the semiclassical approach [12,13]. By applying this concept and re-arranging the field equations for this setting as follows:

$$R_{\mu\nu} - \frac{1}{2}Rg_{\mu\nu} - \frac{R\mathscr{R}_{\mu\nu}}{\mathscr{R}} = \frac{8\pi G_{\mathscr{R}}}{c^4}\hat{T}_{\mu\nu} - \frac{R\left(\mathscr{K}_{\mu\nu} - \frac{1}{2}K\hat{p}_{\mu\nu}\right) - \mathscr{R}\left(K_{\mu\nu} - \frac{1}{2}K\hat{q}_{\mu\nu}\right)}{\mathscr{R}} = 0 \quad (6)$$

From Equation (6), the field equations yield:

$$R_{\mu\nu} = \frac{1}{2}Rg_{\mu\nu} + \frac{R\mathscr{R}_{\mu\nu}}{\mathscr{R}} = \frac{1}{2}R\left(g_{\mu\nu} + 2\widetilde{g}_{\mu\nu}\right) = \frac{1}{2}Rg_{\mu\nu}\left(1 + 2\Omega^2\right) == \frac{1}{2}R\hat{g}_{\mu\nu}0 \quad (7)$$

where Ω^2. is a conformal function relating the bulk and cloud-world metrics as $\widetilde{g}_{\mu\nu} = g_{\mu\nu}\Omega^2$. The conformally transformed metric $\hat{g}_{\mu\nu} = g_{\mu\nu}\left(1 + 2\Omega^2\right)$ can be expressed as:

$$ds^2 = -A(r)\left(1 + 2\Omega^2(r,\widetilde{r})\right)c^2dt^2 + S^2\left(B(r)\left(1 + 2\Omega^2(r,\widetilde{r})\right)dr^2 + r^2d\theta^2 + r^2sin^2\theta\, d\phi^2\right) \quad (8)$$

where A and B are functions of the cloud-world radius r, whereas Ω^2 is a function of the bulk radius of curvature $\widetilde{r}$ and it can be influenced by the cloud-world radius. S^2 is a dimensionless conformal scale factor. By performing the coordinate transformation as:

$$ds^2 = -\left(A(\lambda) + 2A(\lambda)\Omega^2(\lambda,\curlyvee)\right)c^2dt^2 + \left(B(\lambda) + 2B(\lambda)\Omega^2(\lambda,\curlyvee)\right)d\lambda^2 + \lambda^2d\theta^2 + \lambda^2sin^2\theta\, d\phi^2 \quad (9)$$

The Christoffel symbols of this metric are:

$$\begin{gathered}\Gamma^1_{00} = \frac{\dot{A}\left(1+2\Omega^2\right)+4A\dot{\Omega}}{2\left(B+2B\Omega^2\right)},\ \Gamma^0_{01} = \frac{\dot{A}\left(1+2\Omega^2\right)+4A\dot{\Omega}}{2\left(A+2A\Omega^2\right)},\ \Gamma^1_{11} = \frac{\dot{B}\left(1+2\Omega^2\right)+4B\dot{\Omega}}{2\left(B+2B\Omega^2\right)} \\ \Gamma^1_{22} = \frac{-\lambda}{\left(B+2B\Omega^2\right)},\ \Gamma^1_{33} = \frac{-\lambda sin^2\theta}{\left(B+2B\Omega^2\right)},\ \Gamma^2_{21} = \Gamma^2_{12} = \frac{1}{\lambda} \\ \Gamma^2_{33} = -sin\theta\, cos\theta\ ,\ \Gamma^3_{32} = \Gamma^3_{23} = \frac{cos\theta}{sin\theta}\end{gathered} \quad (10)$$

The Ricci tensor components are:

$$\begin{gathered}R_{tt} = -\frac{\ddot{A}\left(1+2\Omega^2+4\dot{\Omega}\right)+4A\ddot{\Omega}+4\dot{\Omega}\dot{A}}{2\left(B+2B\Omega^2\right)} + \frac{\left(\dot{A}\left(1+2\Omega^2\right)+4A\dot{\Omega}\right)\left(\dot{B}\left(1+2\Omega^2\right)+4B\dot{\Omega}\right)}{4\left(B+2B\Omega^2\right)^2} \\ + \frac{\left(\dot{A}\left(1+2\Omega^2\right)+4A\dot{\Omega}\right)^2}{4\left(A+2A\Omega^2\right)\left(B+2B\Omega^2\right)} - \frac{1}{\lambda}\frac{\dot{A}\left(1+2\Omega^2\right)+4A\dot{\Omega}}{\left(B+2B\Omega^2\right)}\end{gathered} \quad (11)$$

$$\begin{gathered}R_{rr} = \frac{1}{2}\left(\frac{\ddot{A}\left(1+2\Omega^2+4\dot{\Omega}\right)+4A\ddot{\Omega}+4\dot{\Omega}\dot{A}}{\left(A+2A\Omega^2\right)} - \frac{\left(\dot{A}\left(1+2\Omega^2\right)+4A\dot{\Omega}\right)^2}{2\left(A+2A\Omega^2\right)^2}\right) \\ - \frac{\left(\dot{A}\left(1+2\Omega^2\right)+4A\dot{\Omega}\right)\left(\dot{B}\left(1+2\Omega^2\right)+4B\dot{\Omega}\right)}{4\left(A+2A\Omega^2\right)\left(B+2B\Omega^2\right)} - \frac{1}{\lambda}\frac{\dot{B}\left(1+2\Omega^2\right)+4B\dot{\Omega}}{B+2B\Omega^2}\end{gathered} \quad (12)$$

$$R_{\theta\theta} = \frac{1}{\left(B + 2B\Omega^2\right)} - \frac{\lambda}{2\left(B + 2B\Omega^2\right)}\left(\frac{\dot{B}\left(1 + 2\Omega^2\right) + 4B\dot{\Omega}}{\left(B + 2B\Omega^2\right)} - \frac{\dot{A}\left(1 + 2\Omega^2\right) + 4A\dot{\Omega}}{\left(A + 2A\Omega^2\right)}\right) - 1 \quad (13)$$

$$R_{\phi\phi} = \frac{sin^2\theta}{\left(B + 2B\Omega^2\right)} - \frac{\lambda sin^2\theta}{2\left(B + 2B\Omega^2\right)}\left(\frac{\dot{B}\left(1 + 2\Omega^2\right) + 4B\acute{\Omega}}{\left(B + 2B\Omega^2\right)} - \frac{\dot{A}\left(1 + 2\Omega^2\right) + 4A\dot{\Omega}}{\left(A + 2A\Omega^2\right)}\right) - sin^2\theta \quad (14)$$

where the dot sign represents a total derivative of the function.

Substituting the Ricci tensor components in Equations (11)–(14) to Equation (7) gives:

$$\left(\dot{A}\left(1+2\Omega^2\right)+4A\dot{\Omega}\right)\left(B+2B\Omega^2\right)+\left(A+2A\Omega^2\right)\left(\dot{B}\left(1+2\Omega^2\right)+4B\dot{\Omega}\right)=0 \quad (15)$$

Equation (15) yields:

$$B+2B\Omega^2=\frac{k}{A+2A\Omega^2} \quad (16)$$

where $k=1+4\Omega^2+\Omega^4$ denotes the conformal metric by considering the bulk curvature.

The weak-field limit, $\hat{g}_{\mu\nu}\approx\eta_{\mu\nu}+\hat{h}_{\mu\nu}$, is applied as follows:

$$\Gamma^i_{tt}=\frac{1}{2}\int\partial_i\hat{h}_{tt}=\frac{1}{c^2}\int\partial_i\varphi \quad (17)$$

where φ is the Newtonian gravitational potential. Both sides are integrated:

$$\hat{g}_{tt}=-A\left(1+2\Omega^2\right)=-\left(\eta_{tt}+\frac{2\varphi_c}{c^2}+\frac{2\varphi_p}{c^2}\right) \quad (18)$$

where $\varphi_c=-GM/\lambda$ is the gravitational potential of the cloud-world's spherical mass and φ_p that arises from the integration can be interpreted as the gravitational potential that results from the bulk curvature, which could be expressed, using the same Newtonian analogue, in terms of the mass, M_p, of the early Universe plasma of a preferred positive curvature and the bulk curvature radius ר as $\varphi_p=-G_pM_p/\text{ר}$. The metric should yield only the gravitational potential of the cloud-world when there is neither a bulk curvature $\left(\Omega^2=0\right)$ nor bulk potential ($\varphi_b=0$). Accordingly, $A=\left(1+2\varphi_c/c^2\right)$; consequently, the conformal function is $\Omega^2=\varphi_p/Ac^2$. By performing the coordinate re-transformation of the metric and combining Equations (16)–(18), which yield:

$$\Omega^2=-\frac{G_pM_p}{\text{ר}c^2}\left(1-\frac{2GM}{rc^2}\right)^{-1},\qquad A=1-\frac{2GM}{rc^2},\qquad B=\left(1-\frac{2GM}{rc^2}\right)^{-1} \quad (19)$$

where the conformal function Ω^2 relies on the gravitational potential of the bulk while its influence is inversely proportional to cloud-world potential. The gravitational potential of the bulk, based on the preferred early Universe positive curvature, decreases with the Universe expansion, and vanishes in the flat spacetime background ($\text{ר}\to\infty$). The minus sign of Ω^2 reveals a spatial shrinking through evolving in the conformal time, which agrees with the vortex model that can occur due to high-speed spinning of the core. By substituting Equation (19) to Equation (8), the conformally transformed metric $\hat{g}_{\mu\nu}=g_{\mu\nu}+2\widetilde{g}_{\mu\nu}=g_{\mu\nu}\left(1+2\Omega^2\right)$ is:

$$ds^2=\left(1-\frac{r_s}{r}-\frac{\text{ר}_p}{\text{ר}}\right)\left(-c^2dt^2+S^2\left(\frac{dr^2}{1+\frac{r_s{}^2}{r^2}-2\frac{r_s}{r}}+\frac{r^2d\theta^2+r^2sin^2\theta d\phi^2}{1-\frac{r_s}{r}-\frac{\text{ר}_p}{\text{ר}}}\right)\right) \quad (20)$$

This metric reduces to the Schwarzschild metric in a flat background ($\text{ר}\to\infty$), where ר is the background or the bulk curvature radius, r_s is the Schwarzschild radius, $\text{ר}_p=2G_pM_p/c^2$ is the early Universe gravitational radius and S^2 is a dimensionless spatial scale factor. The denominator of the radial dimension can be interpreted as an intrinsic curvature term where the metric on the radial and two-sphere is warped by the bulk and cloud-world radii. The metric can be visualized through evolving in the conformal time by using Flamm's approach as follows:

$$w(\mathfrak{r},r)=\mp\int\frac{\sqrt{\left(\frac{r_s}{r}-\frac{r_s{}^2}{r^2}-\frac{\text{ר}_p}{\text{ר}}\right)}}{\left(1-\frac{r_s}{r}\right)}\,dr=\mp\sqrt{r_s(r-r_s)-\text{ר}_p\frac{r^2}{\text{ר}}}+\mathcal{O}+C \quad (21)$$

where C is a constant and $\mathcal{O}$ denotes less significant terms.

While the minus sign of Ω^2 reveals a spatial shrinking through evolving in the conformal time, which agrees with the vortex model, the positive and negative solutions of Equation (21) indicate that the evolution is in opposite directions. This means that the central event horizon is leading to opposite vortices (traversable wormholes). According, the accretion flow into the supermassive compact object only occurs at the central event horizon of the two opposite vortices while their other ends eject the relativistic jets as shown in Figure 1.

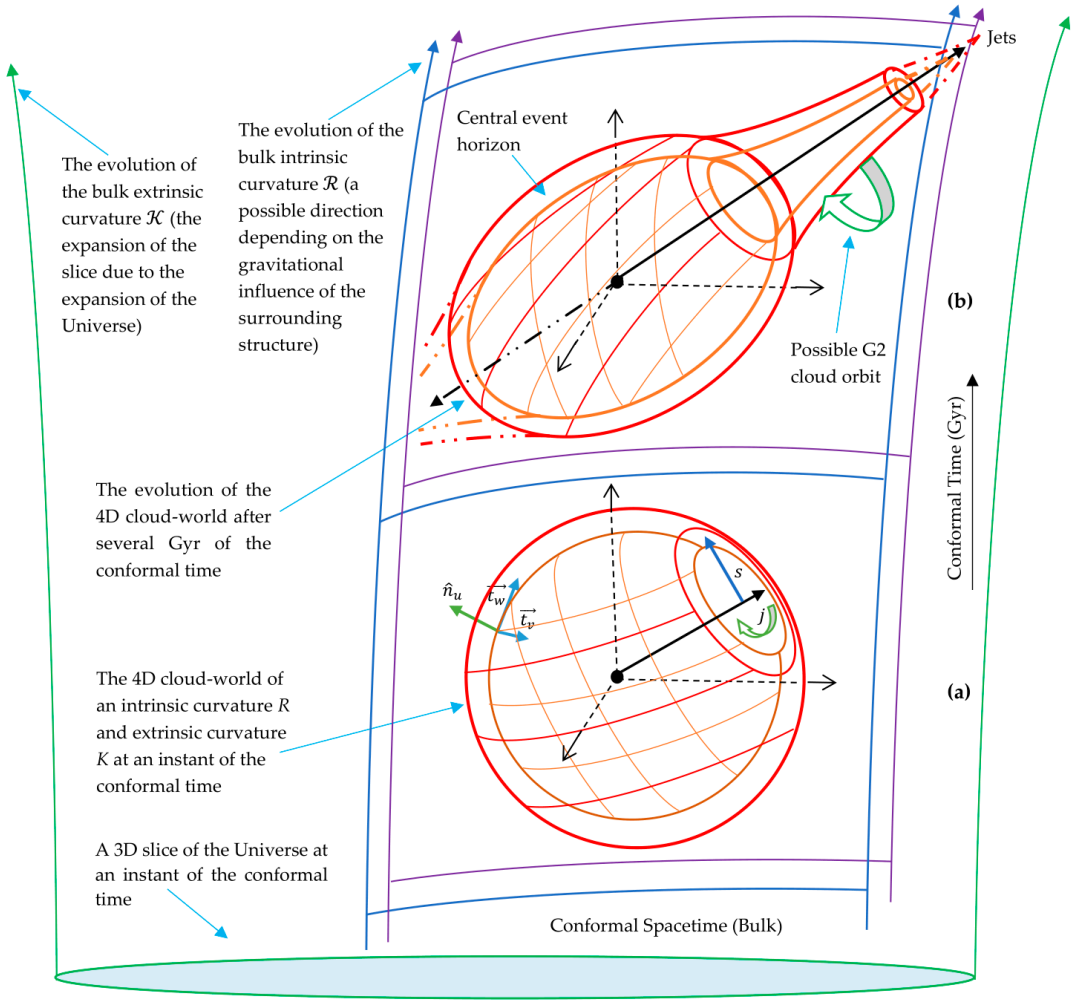

Figure 1. The hypersphere of a compact core of a galaxy (the red-orange 4D cloud-world) along with its travel and spin through the conformal spacetime (the blue-purple 4D bulk representing the bulk of distinctive curvature evolving over the conformal time.

To evaluate the influence of the spinning and the curvature of the bulk on the core of the galaxy and the surrounding gas clouds (the spiral arms), a fluid simulation was performed based on Newtonian dynamics by using the Fluid Pressure and Flow software [14]. In this simulation, the fluid was deemed to represent the spacetime continuum throughout incrementally flattening curvature paths representing conformal curvature evolution to analyze the external momenta exerted on objects flowing throughout the incrementally flattening curvatures. The momenta yielded by the fluid simulation were used to simulate a spiral galaxy as a forced vortex as shown in Figure 2.

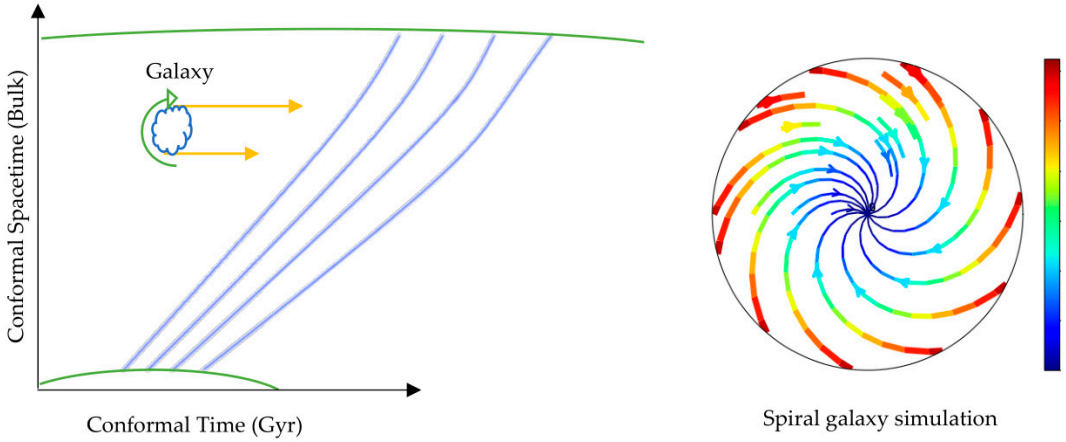

Figure 2. (**a**) External fields exerted on a galaxy due to the spacetime conformal curvature evolution. Green curves represent the curvature of spacetime worldlines. Blue curves represent the simulated spacetime continuum. (**b**) Simulation of spiral galaxy rotation. Blue represents the slowest tangential speeds and red represents the fastest speeds which could resemble observations of galaxy rotation except the simulation used an ideal fluid.

The simulation shows that the tangential speeds of the outer parts of the spiral galaxy are rotating faster in comparison with the rotational speeds of the inner parts, which could resemble observations of galaxy rotation except the simulation used an ideal fluid.

4. Conclusions and Future Works

In this study, interaction field equations are derived in which the curvature of the background or the 4D conformal bulk evolves over the conformal time based on the PL18 recent release which has preferred a positively curved early Universe with a confidence level higher than 99%. Throughout this bulk, 4D relativistic cloud-worlds flow and spin.

Owing to the curved background, these findings of galaxy formation showed that the core of the galaxy undergoes a forced vortex formation with a central event horizon leading to opposite traversable wormholes that are spatially shrinking through evolving in the conformal time. It revealed that the galaxy and its core form in the same process, while the surrounding gas clouds can form spiral arms due to the fast-rotating core. These findings demonstrated that the accretion flow onto the central supermassive compact object only occurs at the central event horizon of the two opposite vortices while their other ends eject the relativistic jets. This can elucidate the relativistic jet formation and the G2 gas cloud motion if its orbit is around one of the vortices but at a distance from the central event horizon. The gravitational potential of the early curved bulk contributes to galaxy formation while the present spatial flatness deprives the bulk potential which could contribute to galaxy quenching. The formation of the galaxy and its core at the same process can explain the formation of supermassive compact galaxy cores with a mass of ~10^9 $M_\odot$ at just 6% of the current Universe age and could solve the black hole hierarchy problem.

Funding: This research received no external funding.

Institutional Review Board Statement: Not applicable.

Informed Consent Statement: Not applicable.

Data Availability Statement: Not applicable.

Conflicts of Interest: The author declares no conflict of interest.

References

1. Beall, J.H. A Review of Astrophysical Jets. *Front. Res. Astrophys. II* **2016**, *mbhe 58*, 53.
2. Kundt, W. A Uniform Description of All the Astrophysical Jets. *PoS (FRAWS 2014)* **2014**, *25*, 1–9.
3. Beall, J.H. A review of astrophysical jets. In *Frascati Workshop 2013, Proceedings of the Tenth International Workshop on Multifrequency Behaviour of High Energy Cosmic Sources Palermo, Italy, 2013*; Naval Research Laboratory: Washington, DC, USA, 2014; pp. 259–264.
4. Di Valentino, E.; Melchiorri, A.; Silk, J. Planck evidence for a closed Universe and a possible crisis for cosmology. *Nat. Astron.* **2020**, *4*, 196–203. [CrossRef]
5. Mokeddem, R.; Hipólito-Ricaldi, W.S.; Bernui, A. 2022 Excess of lensing amplitude in the Planck CMB power spectrum. *J. Cosmol. Astropart. Phys.* **2023**, *1*, 017. [CrossRef]
6. Handley, W. Curvature tension: Evidence for a closed universe. *Phys. Rev. D* **2021**, *103*, L041301. [CrossRef]
7. Linde, A. Can we have inflation with Omega > 1? *J. Cosmol. Astropart. Phys.* **2023**, *2003*, 002. [CrossRef]
8. Efstathiou, G. Is the Low CMB Quadrupole a Signature of Spatial Curvature? *Mon. Not. R. Astron. Soc.* **2003**, *343*, L95–L98. [CrossRef]
9. Landau, L.D. *Theory of Elasticity*; Elsevier: Amsterdam, The Netherlands, 1986.
10. Al-Fadhli, M.B. 2022 Celestial and Quantum Propagation, Spinning, and Interaction as 4D Relativistic Cloud-Worlds Embedded in a 4D Conformal Bulk: From String to Cloud Theory. *Preprints* **2020**, 2020100320. [CrossRef]
11. Kozameh, C.; Newman, E.; Tod, K.P. Conformal Einstein Spaces. *Gen. Relativ. Gravit.* **1985**, *17*, 343–352.
12. Dyer, E.; Hinterbichler, K. Boundary terms, variational principles, and higher derivative modified gravity. *Phys. Rev. D Part. Fields Gravit. Cosmol.* **2009**, *79*, 024028. [CrossRef]
13. Brown, J.D.; York, J.W. Microcanonical functional integral for the gravitational field. *Phys. Rev. D* **1993**, *47*, 1420–1431. [CrossRef] [PubMed]
14. Reid, S.; Podolefsky, H.; Pual, A. *Fluid Pressure and Flow, PhET Interactive Simulations*; University of Colorado: Denver, CO, USA, 2013.